Rock Mechanics
and Rock Engineering 24, 115—132

**Rock Mechanics
and Rock Engineering**

Stress-Strain Fields at the Tunnelling Face — Three-dimensional Analysis for Two-dimensional Technical Approach

By

S. Kielbassa and **H. Duddeck**

Institute for Structural Analysis, Technical University, Braunschweig,
Federal Republic of Germany

Summary

For tunnelling in rock, the original stress field in the ground is changed considerably before a first lining is participating in stabilizing the opening. Depending on this stress release at the tunnel face, only a small portion of the primary stresses is acting on the lining. Only a three-dimensional approach is able to determine the stresses and the deformations of the ground and the lining realistically. The paper presents some results of elastic three-dimensional finite-element-analyses in consecutive steps of the sectional excavation of circular and non-circular tunnels. From these results an equivalent two-dimensional approach is derived for technical applications, given in diagrams.

1. Introduction

Figure 1 shows the characteristic difference of a simplified two-dimensional appraoch (plane strain model) and the actual development of the crown deformations with excavation advance. If the full primary stresses are applied to a plane system which includes also the full strength of the supporting lining, the analysis yields stresses corresponding to $w^{NL} - w^{2d}$ in Fig. 1, which are unrealistically large compared to those corresponding to w^e of the three-dimensional analysis. In Fig. 1, $w_1^p + w_2^p$ are the predeformations resulting from stress release ahead of the lining. The curves in Fig. 1 are, of course, different with the length of the open section l_u, with the developing strength of the lining, and so on.

The plane design model is an upper-limit model with respect to stresses in the lining. It may be more valid the softer the ground is, see e. g. the ITA Guide lines (1988). Yet, it is a lower limit model for analysing the ground. It does not cover the release of ground stresses radial to the tunnel lining and at the opening surfaces, which yields greater deviatoric states of stresses, hence more failure prone cases. Therefore, a three-dimensional analysis is indispensable for tunnel excavations in rock and medium soft ground, where e. g. shotcreting and rock bolting is applied for first support.

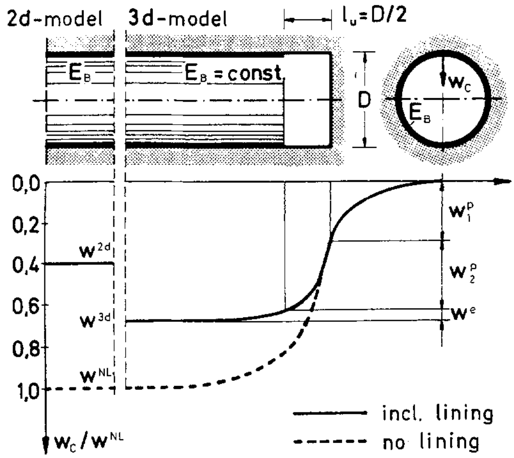

Fig. 1. Relative displacement of the crown; left: two-dimensional model, right: development with excavation advance by applying a three-dimensional model, s. Erdmann (1983)

However, a three-dimensional approach is in general not suited for the practical tunnelling engineer, because of too costly an analysis, and perhaps it may even be inconsistent with respect to the overall accuracy obtainable in view of usually rough estimates of important ground characteristics. Tunnelling practice is therefore asking for simpler technical approaches, as those applying only two-dimensional design models, see ITA-Guide lines (1988), also Duddeck and Erdmann (1985). That is the reason why the paper presented here is proposing a two-dimensional approach which nevertheless is covering the more relevant features of a three-dimensional theory. Although papers on three-dimensional, also non-linear analyses have been published before, see e. g. Baudendistel (1979), Semprich (1980), Berwanger (1985), Swoboda (1988), a renewed attempt is justified not only because of more computational facilities available in the meantime. The main results presented here are based on Kielbassa (1989).

2. Three-dimensional Analysis for the Advancing Tunnelling Face

In tunnelling, the ground responses to each round of excavation (e. g. after blasting) by a release of the stresses normal to open surfaces and by corresponding inward displacements. Assuming that the ground is sufficiently homogeneous along the tunnel axis, the effects of each blasting round add up to a state of stresses and deformations, which after some rounds has finally the same pattern for each advance step.

For covering this behaviour by a three-dimensional finite-element-analysis, it proved to be most efficient by following the advance by an element mesh as shown in Fig. 2. If the vector of the stresses and deformations is Z_e^t at the time or excavation phase t for the finite element e and an incremental change is ΔZ_e^t, then the superposition due to the advancing mesh yields:

$$Z_e^t = Z_{e+1}^{t-1} + \Delta Z_e^t, \quad e = 1\ldots(n-1). \tag{1}$$

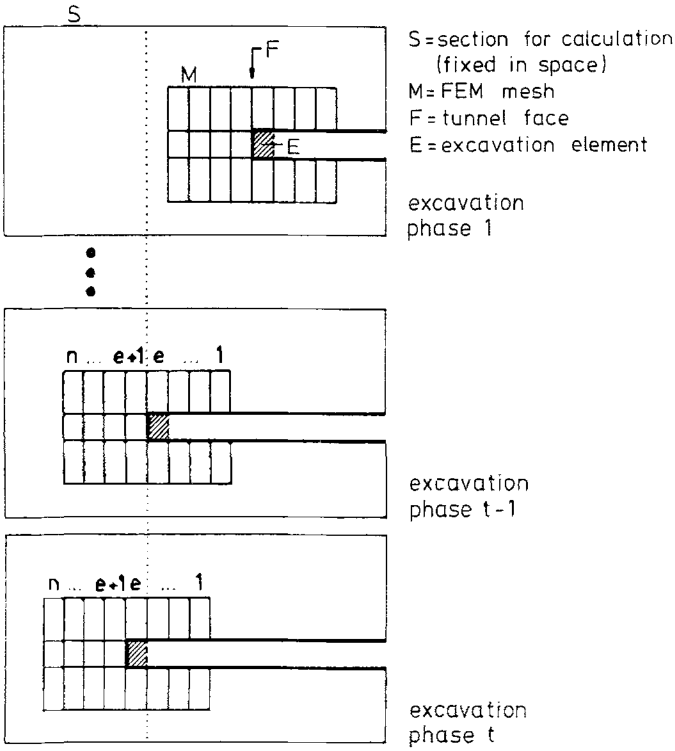

Fig. 2. Numerical simulation of the excavation advance by a simultaneously advancing finite-element-mesh, where the length of an excavation round is equal to the width of the corresponding finite element or a manifold of it

For the elements which are presenting the lining, it is necessary to set their stresses equal to zero along that part of the tunnel at the face which is not supported by the lining. After some advance steps a stationary state will be the result. By repeating this procedure, as given in Fig. 3, also more refined tunnelling methods can be simulated numerically, as e. g. those for top heading, followed up in some distances by excavating the bench and farther at the invert. For more information see Kielbassa (1989).

The characteristic pattern for the ring forces N in the lining at the invert and for the crown displacement w (and also their incremental increases ΔN or Δw caused by one advance round) are shown in Fig. 4.

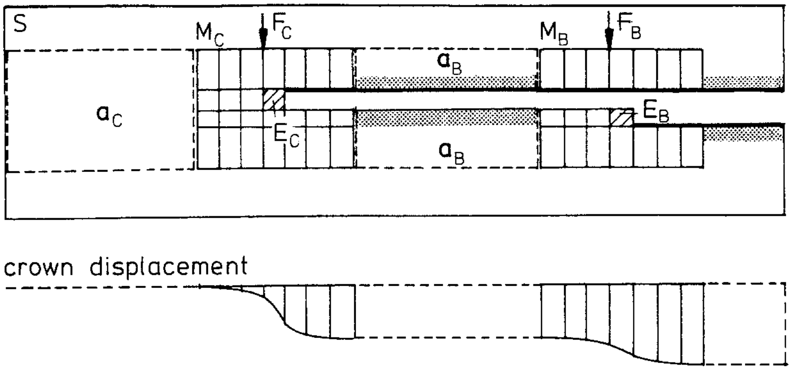

Fig. 3. Numerical procedure with a follow-up finite-element-mesh for sectional excavations: here top heading (calotte) at M_c and bench excavation at M_B. S, F, E see Fig. 2, a is the area outside the travelling mesh

Along the open section immediately at the face the Δw-values show a typical maximum which has the result that the incremental ring forces N are maximum at the very edge of the lining (assumed in Fig. 4 as having immediate full strength) and that ΔN declines with the distance from the face. The pattern of sagging curves of the total displacements and ring forces is obtained after calculation of some excavation advances (nine in Fig. 4). This pattern results from the time dependent interactive behaviour of the ground-lining-structure (not caused by numerical oscillations). It is not recorded by in-situ-measurements, since usually only one reading device is installed within one advance field. Displacement measurements inside the tunnel cannot cover the preceding part of deformations. However, more refined measurements by Baumann (1988) have verified the hoop force pattern of Fig. 4.

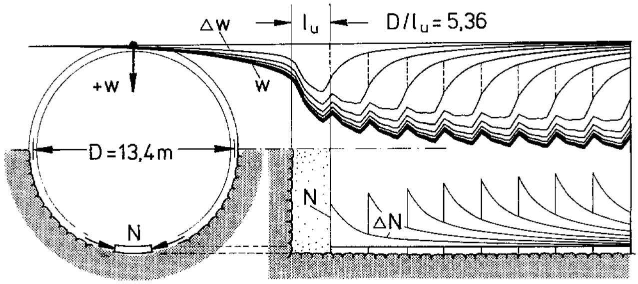

Fig. 4. Pattern of the ring forces N and the crown displacements after some advance rounds for a full face excavation of a circular tunnel cross section

Utilizing symmetry, the applied step by step progressing finite-element mesh has the dimensions like that in Fig. 5. For the three-dimensional finite element an isoparametric hexaedron of 20 nodes (quadratic shape functions) is chosen. For the numerical evaluation the FE-programme ADINA has been applied in an extended version including some features specific to the tunnel advance problem. For the applications in section 4 of this paper, ground and lining are assumed to behave elastically although nonlinear algorithms are available in the programme.

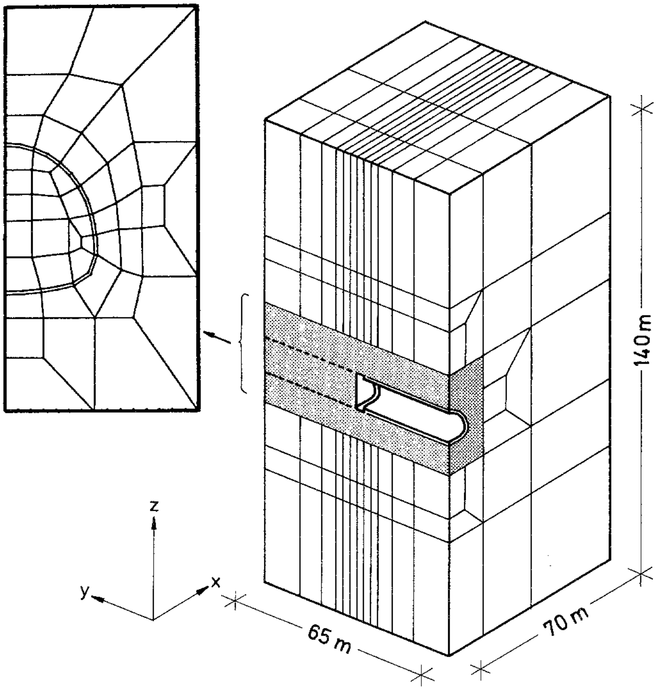

Fig. 5. Applied travelling FEM-mesh for a noncircular tunnel cross with invert concrete

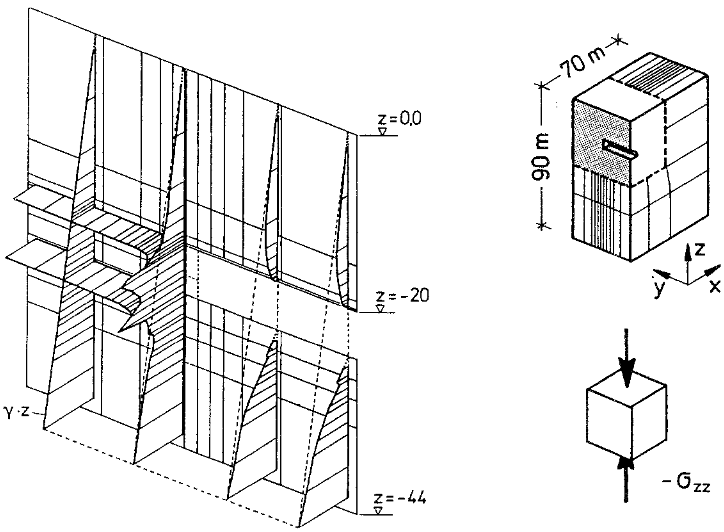

Fig. 6. Distribution of the vertical stresses in the symmetry plane after top heading excavation

An example of the results is shown in Fig. 6. The mesh for the top-heading covers three horizontal layers of different ground and has 664 elements with 3348 nodes and 8675 unknowns. The stress distribution of Fig. 6 very well shows the endangered section very close to the face.

A more local view of the stresses close at the face is presented in Fig. 7. The stress release below the tunnel invert and the very local arch effect spanning the open section l_u are clearly visible, see also Fig. 4. The initial stress pattern is preserved throughout the following advance rounds, even if the lining is fully activated. However, this local pattern is evaluated only, when a more refined finite element mesh is chosen. Figure 8 shows the stress distributions in some horizontal lines below the tunnel invert of Fig. 7 for two different meshes. The arching effects close to the open section is showing up only when this section is divided into four elements (not, of course, when one round is equal to one element). Hence, the evaluated stresses in the lining in longitudinal direction, especially those by bending of the lining, are also very much influenced by the chosen refinement of the finite-element-mesh. The stresses in the ring direction of the lining are less effected, see Kielbassa (1989), and their mean values over one round length calculated by differently refined meshes coincide well.

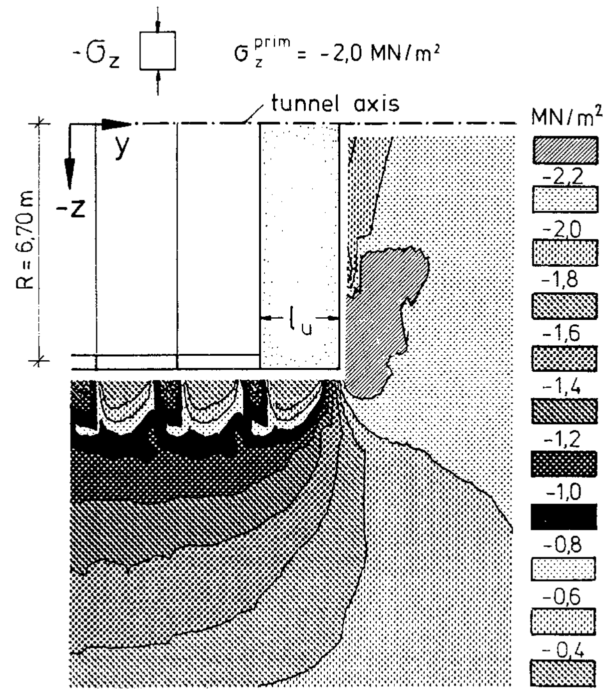

Fig. 7. Vertical stresses (iso-lines) around the open face (length l_u) of a circular tunnel in the lower half of the vertical symmetry plane

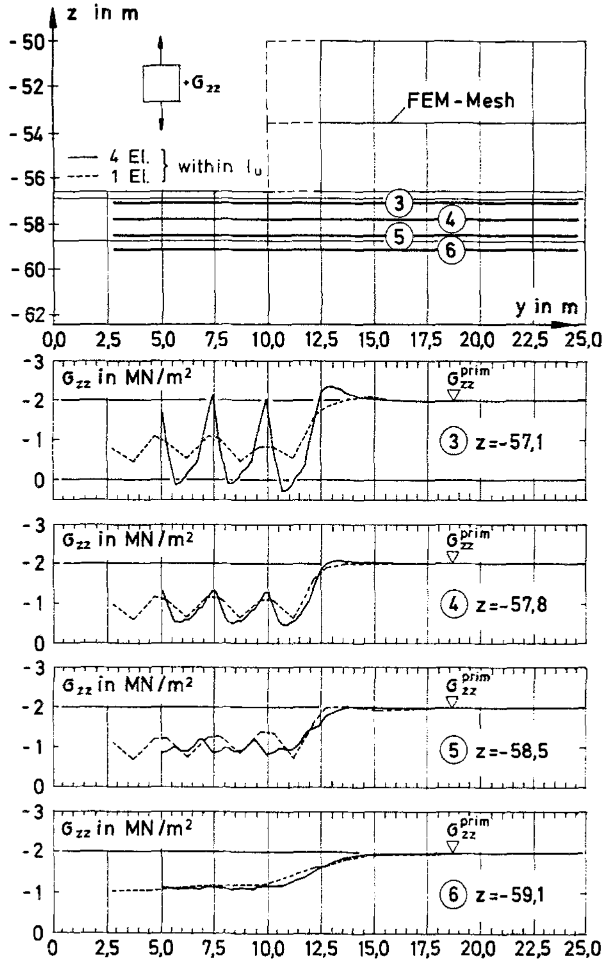

Fig. 8. Stresses along the lines 3 to 6 below the tunnel invert for .... one element and —— four elements within the 2.5 m excavation round, see also Fig. 7

3. Comparison with Results of Two-dimensional Models

Two-dimensional design models may be valid primarily only for soft soil tunnelling, e. g. for shielddriven tunnels, see ITA-Guide-lines (1988). Here it may be assumed that due to the rigidity of the shield machine rather small predeformations occur before the lining is effective. Yet, the straightforward two-dimensional model yields deformations too small and lining stresses too large. For technical applications it is desirable to reduce a three-dimensional approach, which considers partial stress release at the tunnelling face, to a two-dimensional model. In Fig. 9 the very pronounced difference is explained by the convergence-confinement curves, here linearized. The radial ground pressure may be released completely by inward deformations of w^{NL}. The stiffness of the lining — here by considering

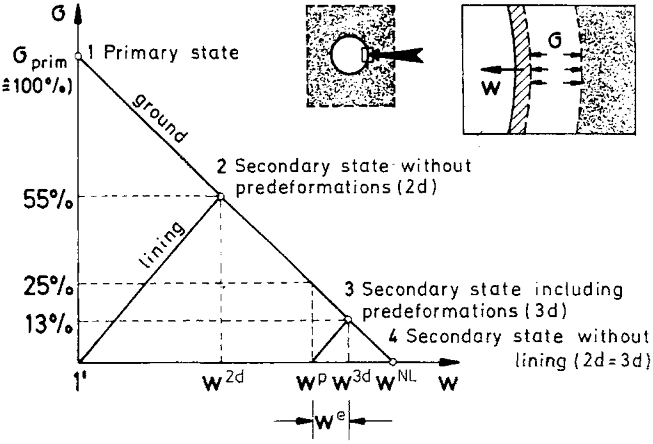

Fig. 9. Simplified characteristics of the reactions of ground and lining to tunnelling

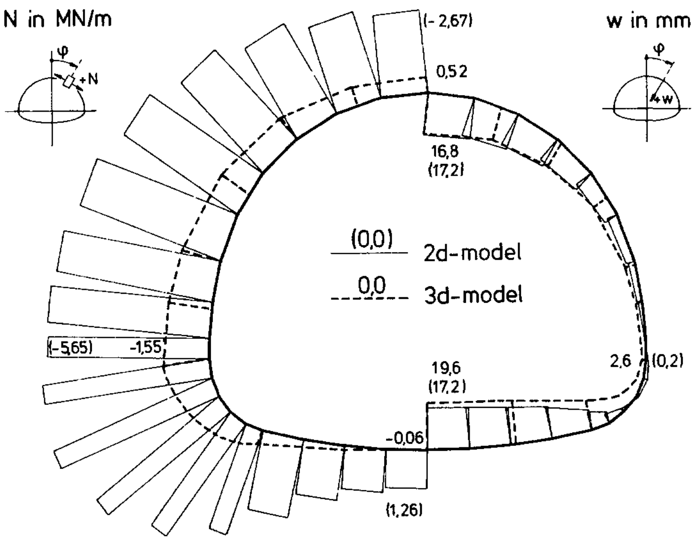

Fig. 10. Ringforces N (left) and radial deformations w for a horseshoe-type tunnel cross section evaluated by a two-dimensional and a three-dimensional approach for a full face excavation, Kielbassa (1989)

radial displacements only — is determining the gradient of the lining characteristic. A two-dimensional model, assuming that the lining is already present when the tunnelling deformations start, would yield, that equilibrium between ground pressure and lining resistance is reached, when inward deformations are w^{2d}. In the example of Fig. 9, 55% of the primary ground stresses are acting on the lining. However, when predeformations of w^p are allowed prior to the lining reaction, then only 13% of the primary ground stresses are taken by the lining. In most real cases the curves in Fig. 9 are non-linear, which increases the effect considerably.

For comparison Fig. 10 shows the different results for a two-dimensional approach (larger N-forces, smaller w-deformations) and for a three-dimensional model (smaller N, lager w). The differences are even larger for bending moments.

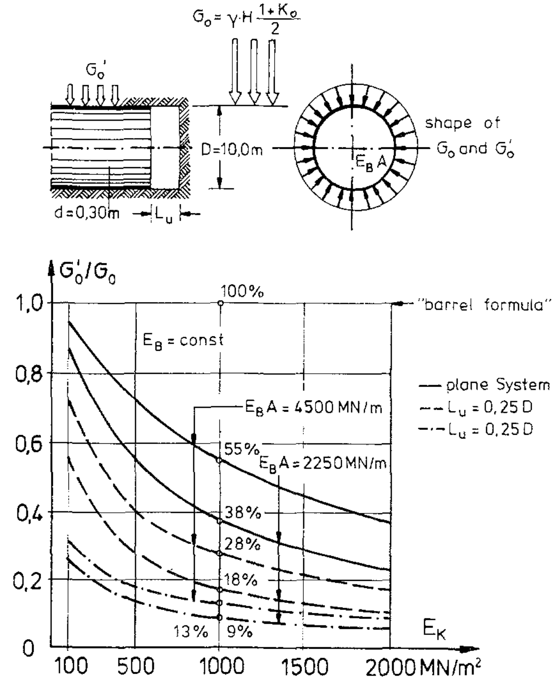

Fig. 11. Effects of stress release for circular cross sections by Erdmann (1983)

A first attempt to derive an equivalent two-dimensional problem via a three-dimensional theory has been made by Erdmann (1983). By applying a rotational three-dimensional model for circular tunnels reduction factors for some selected calculation results were derived. These factors, like those in Fig. 11, allow to reduce certain stresses from 2 d-models to the smaller stresses of the 3 d-model. The example in the figure shows a simplified model, considering only the constant part of the radial pressure for two ring stiffnesses $E_B A$ and two lengths l_u of the open section at the face. The percentages given in Fig. 11 are belonging to a ground stiffness $E_K = 1000$ MN/m². Even in the unrealistic case when the full primary stress is applied simultaneously on the ground opening and the lining, only 55% of the stress is taken by the lining (see also Fig. 9); in the case $E_B A = 2.250$ MN/m, only 38% is acting on the lining. If an open face length $l_U = 0{,}25$ of the tunnel diameter D is left without any support, then the lining takes only 25% of the primary stresses, or even only 13% for $l_U = 0{,}5\ D$ (see also Fig. 9). For $E_B A = 2.250$ MN/m, the values are even smaller, down to 9%. The work of Baudendistel (1979) presents only two values (see Fig. 11) independent from stiffness-relations of ground and lining. Schwartz and Einstein (1978) are also giving percentages only for special cases.

4. Two-dimensional Models Covering the Three-dimensional Approach

In order to provide engineers for the practical design of tunnels with simpler approaches, the results of a consistent three-dimensional model (see Fig. 6) may also be obtained from an equivalent two-dimensional model. This is visualized in Fig. 12, where only the effective ground pressure is relevant for the design of the lining.

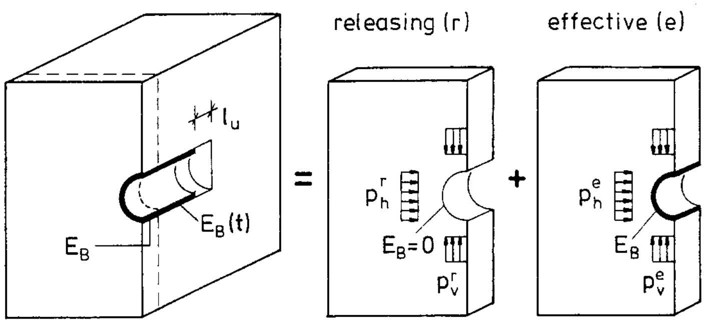

Fig. 12. The results of a complete three-dimensional approach are split into two parts: stress release (r) and effective ground pressure acting on the lining

While conventional ("one step") plane models are applying excavation loads equal to the primary field of ground stresses:

vertical:

$$p_v = \sigma_v^{\text{prim}},$$

horizontal:

$$p_h = \sigma_h^{\text{prim}} = k_0 \cdot p_v, \tag{2}$$

for "two step" plane models according to Fig. 12 these loads are split into two parts. Such models were published by Baudendistel (1979) and Schikora (1982) and used in practical applications as shown by Haberl and Haugeneder (1984), Baumann (1985) and other authors. Yet consistent splitting factors are unknown. In this paper four coefficients: s_v^r, s_v^e and k_r^0, k_e^0 are introduced:

$$p_v^r = s_v^r \cdot \sigma_v^{\text{prim}}, \qquad p_v^e = s_v^e \cdot \sigma_v^{\text{prim}}, \tag{3}$$

$$p_h^r = k_0^r \cdot p_v^r, \qquad p_h^e = k_0^e \cdot p_v^e, \tag{4}$$

where the upper indices mark the stress release part (r) acting on the unlined opening, and the effective groundpressure part (e) acting on the composite system of ground and lining.

For the evaluation of the coefficients from 3 d-results, first the average values of the stresses and deformations are determined along the length of one excavation round in the final steady state after the face has proceeded far enough, see Fig. 4. These values are assumed to be constant along the thickness of the equivalent plane strain model. Then, by evaluating that part of the ground pressure corresponding to the hoop forces in the lining, those excavation loads (the effective part of the two-dimensional system) are determined which yield the same ring forces in the lining as the average values of the three-dimensional theory.

The excavation loads for the releasing part (*r*) of the model are derived from the requirement that they cover the complementary deformations, so that the sum of both parts is equal to the deformations of the 3 d-model.

This procedure is firstly applied to tunnels of circular cross sections, following the analysis of Ahrens, Lindner, Lux (1982). Hence, correspondence between hoop forces and effective primary stresses in the first step of the 2 d-model and between deformations and released primary stresses

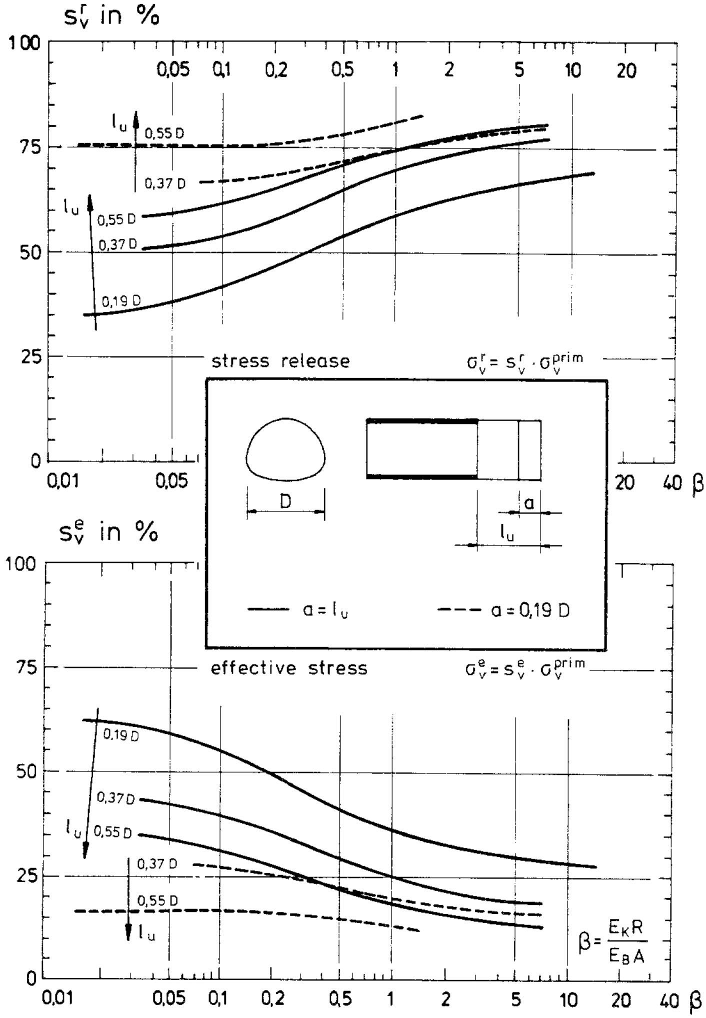

Fig. 13. Primary vertical ground pressure, split up into one part (*r*) corresponding to stress release, and another part (*e*) for effective ground pressures

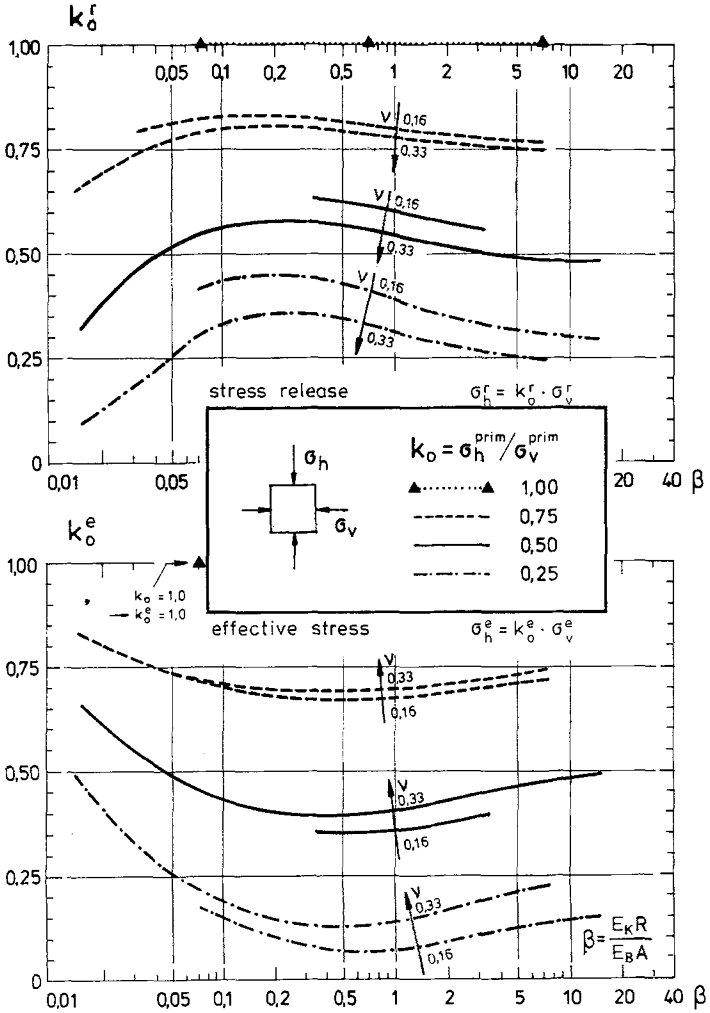

Fig. 14. Primary horizontal ground pressure, split up into a part (r) corresponding to stress release, and another part (e) for effective ground pressures

in its second step is obtained by using the analytical model of an infinite elastic plane with a reinforced circular opening in a primary field of constant stresses (for details see Kielbassa, 1989). Numerical calculations of non-circular tunnel cross sections proved that the reduction rates obtained by applying the procedure as shown in Fig. 12, can also be chosen for horse shoe type cross sections. The error is negligibly small.

Elaborate calculations of many cases for different unlined lengths l_u, lengths a of the excavation round, and different stiffness ratios β, where each case also considers the development of stiffness of the shotcrete, are condensed in Fig. 13 for the equivalent vertical ground pressures and in Fig. 14 for the equivalent horizontal pressures. The horizontal axes of all diagrams represent the stiffness ratio

$$\beta = E_K R / E_B A, \tag{5}$$

where E_K = Young's modulus of the ground,
E_B = Young's modulus of the lining,
R = radius of the upper tunnel cross section,
A = effective area of the lining per unit length along the tunnel axis.

It may be noted, that besides the dependency of β, the diagrams for the vertical stresses (Fig. 13) are depending only on the unlined length l_u, and the length a of an excavation round. Vice versa, the diagrams for the horizontal stresses (Fig. 14), if expressed by the lateral pressure ratio k_0, are influenced only by the k_0-value of the primary stress field and the Poisson's ratio (ν) of the ground.

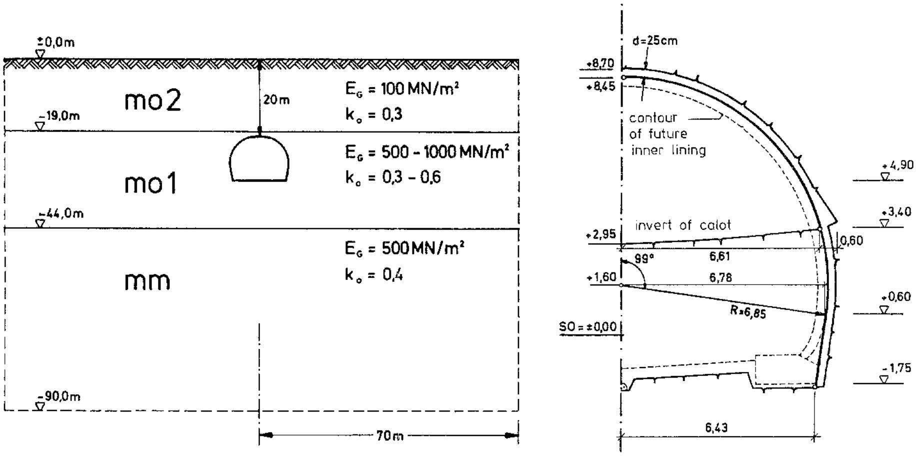

Fig. 15. Example of the application of the solution in equivalent two-step plane models

5. Example Horse Shoe Type Tunnel

Figure 15 outlines an example for the application of the two-step model and the use of the diagrams. The following input data are chosen:

thickness of lining:	d	$= 0.25$ m
area of lining:	A	$= 0.25$ m²/m
radius of lining (centre line):	R	$= 6.85$ m
unsupported length:	l_u	$= 1.70$ m
length of excavation round:	a	$= 1.70$ m
Young's modulus of concrete:	E_B	$= 15\,000$ MN/m²
Young's modulus of rock:		
layer mo2:	E_K	$= 100$ MN/m²
layer mo1:	E_K	$= 500$ MN/m²
specific weight of rock:	γ	$= 0.0245$ MN/m³
height of overburden above the crown:	$H_{\ddot{u}}$	$= 20$ m

Poisson's ratio:	ν	$=$	0.2
ratio of lateral pressure	k_0	$=$	0.3

For applying the diagrams of Fig. 13 and Fig. 14 the procedure is shown in Fig. 16. The following parameters are needed:

lining diameter:	$D = 2R + d$	$= 13.95$ m
dimensionless lengths:	l_u/D	$= 0.12$
	a/D	$= 0.12$
stiffness ratio:	$\beta = E_k R/E_B A$	$= 0.19$ for $E_K = 100$
	β	$= 0.93$ for $E_K = 500$
chosen for design:	β	$= 0.40$ for $E_K = 220$

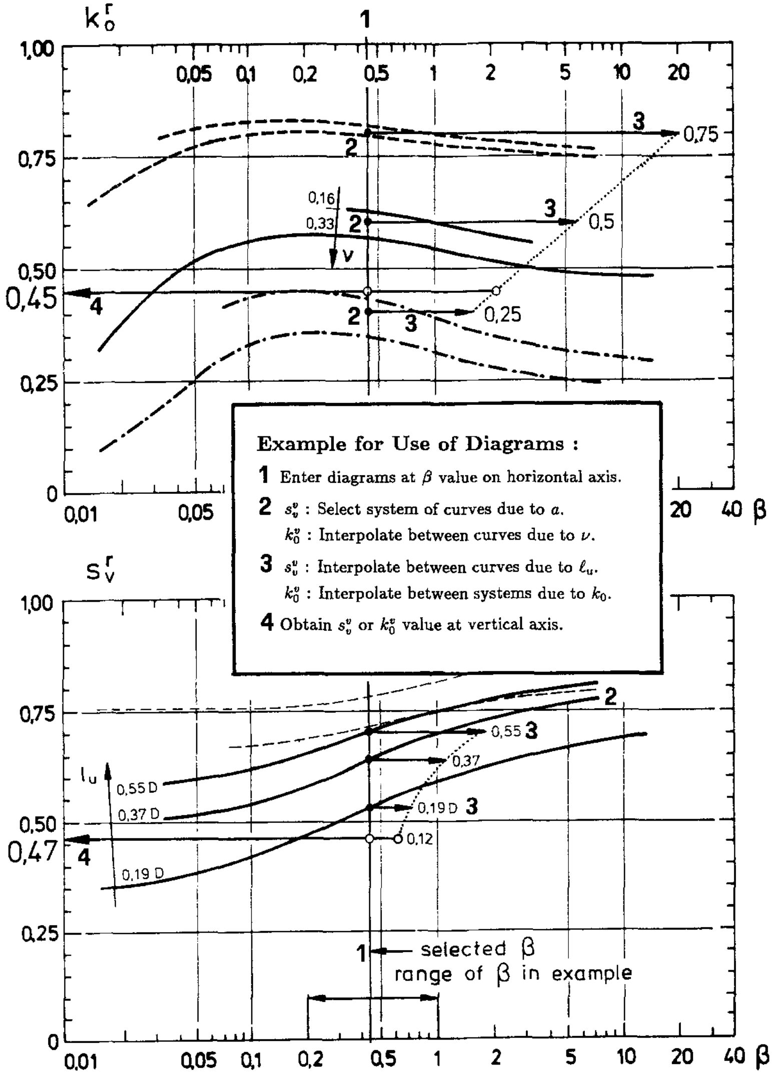

Fig. 16. User's help for diagrams of Fig. 13 and Fig. 14 applied to example in Fig. 15

The design value $\beta = 0.40$ is chosen as an estimated average value by considering the ground layers in Fig. 15. From the diagrams in Fig. 16 it can be seen, that somewhat different values of β do not change the factors much, because of small gradients of the curves.

From Fig. 13 the factors s_v for the vertical pressures are obtained as shown in Fig. 16 for s_v^r: at $\beta = 0.40$ the ordinates of the three curves for $a = l_u$ are used to construct the dotted curve of an interpolation function at

$$l_u/D = 0.185,\ 0.37,\ 0.55,$$

then at $l_u/D = 0.12$, the required splitting factors $s_v^r = 47\%$ and $s_v^e = 49\%$ are found. Note that the sum $s_v^e + s_v^r$ is always less than 100%, the "missing" percentage correspond to the participating strength of the tunnel face.

The lateral pressure ratios k_0^e, k_0^r are obtained analogously from Fig. 14, as shown in Fig. 16 for k_0^r: firstly the influence of Poisson's ratio is introduced by interpolating three times for $\nu = 0.2$ between the curves at $\nu = 0.16$ and $\nu = 0.33$. In these points, which correspond to lateral pressures

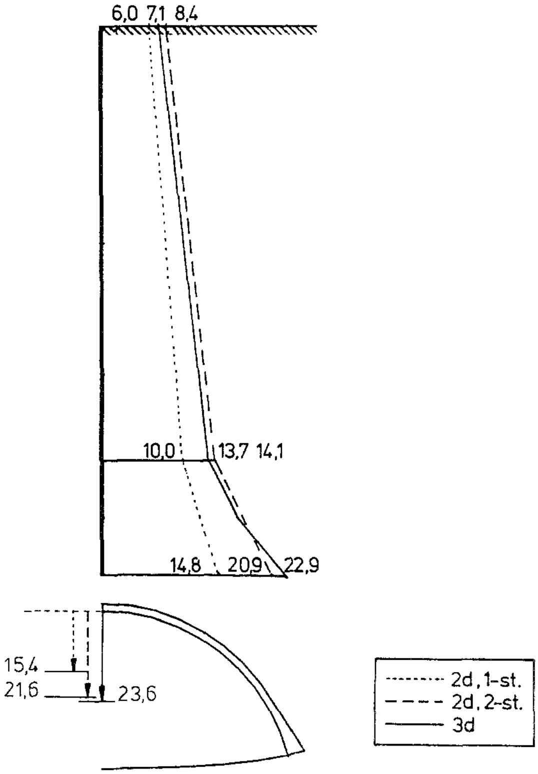

Fig. 17. Downwards displacements of the ground between crown and surface for different design models. $2d$, $1-st$ = usual two-dimensional model, $2d$, $2-st$ = proposed two-step plane model, $3d$ = consistent three-dimensional model

of $k_0 = 0.25$, 0.50, 0.75 in the primary state, the dotted interpolation function is drawn which leads to $k_0^r = 0.45$ for the releasing part and to $k_0^e = 0.15$ for the effective part of the horizontal pressure.

With these values the stresses of the tunnel are evaluated according to Fig. 12 and Eqs. (3), (4) are evaluated as follows: In the first step the tunnel model without lining yields the predeformations and the stress release field given by

$$\gamma^r = \gamma \cdot s_v^r/100\% = 0.0245 \cdot 0,47 = 0.0115 \text{ MN/m}^3, \quad k_0^r = 0.45.$$

The second step yields the stresses in the lining and the corresponding deformations. Therefore, the second model in Fig. 12 with a lined tunnelling opening is evaluated for a stress field of:

$$\gamma^e = \gamma \cdot s_v^e/100\% = 0.0245 \cdot 0.49 = 0.0120 \text{ MN/m}^3, \quad K_0^e = 0.15.$$

Some of the results are shown in Fig. 17 and Fig. 18. For comparison the results of a conventional one-step 2 d-model are also plotted.

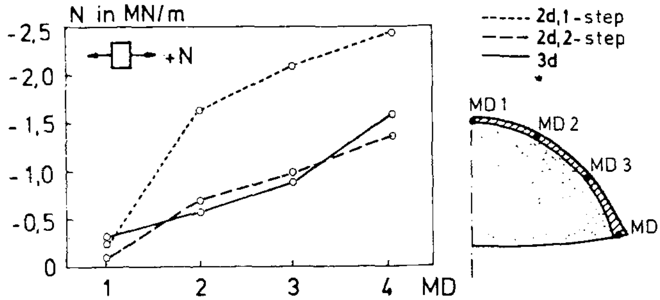

Fig. 18. Ring stresses in the tunnel lining at four cross sections MD1 to MD4 for different design models, see Fig. 16

This example shows, that also for non-circular tunnels close to the ground surface the load splitting factors are applicable. In Table 1 the main parameters of the 3 d-model and the two-step 2 d-model are compared. The considerable reduction of computer ressources (and also man power) by using an equivalent plane model instead of a three dimensional analysis is obvious.

Table 1. Reduction of the computational items of the numerical analysis of the proposed two-step plane model via a consistent three-dimensional approach

	2 d-model	3 d-model
Maximum band width	50	1605
Mean band width	—	957
Number of unknowns	364	10439
Number of nodes	182	4369
Number of elements	294	808
CPU time (sec)	5	7500

6. Concluding Remarks

The determination of stresses and deformations of a tunnel structure is certainly a complex problem depending on many influences of the ground as well as of the excavation procedure. A simplified two-steps plane model approach is proposed, derived from a complete three-dimensional model with advancing tunnelling face. Hereby, it is hoped that the most important effect of stress release (before the lining resistance is activated) is at least approximately taken into account more realistically than hitherto. The approach is the more relevant the stiffer the ground is.

References

Ahrens, H., Lindner, E., Lux, K.-H. (1982): Zur Dimensionierung von Tunnelausbauten nach den Empfehlungen zur Berechnung von Tunneln in Lockergestein. Bautechnik 8, 260—273 and 9, 303—311.

Baudendistel, M. (1979): Zum Entwurf von Tunneln mit großen Ausbruchsquerschnitt. Rock Mechanics, Suppl. 8, 75—100.

Baumann, T. (1988): Numerical analysis and reality in tunnelling-verification by measurements? In: Proc., Num. Methods in Geomechanics, Innsbruck, Balkema, Rotterdam, 1457—1464.

Baumann, T., Sulke, B.-M., Trysna, T. (1985): Einsatz von Messung und Rechnung bei Spritzbetonbauweisen im Lockergestein. Bautechnik 10, 330—337 and 11, 368—374.

Berwanger, W.: Dreidimensionale Berechnung von tiefliegenden Felstunneln unter Berücksichtigung des rheologischen Verhaltens von Spritzbeton und des Bauverhaltens. Forschungsergebnisse aus dem Tunnel- und Kavernenbau, H. 10, Universität Hannover.

Duddeck, H., Erdmann, J. (1985): On structural design models for tunnels in soft soil. Underground Space 9, 245—259.

Erdmann, J. (1983): Comparison of plane and development of 3-dimensional analyses for tunnelling (in German). Report Nr. 83-40. Institut für Statik, Technische Universität Braunschweig.

Haberl, E., Haugeneder, E. (1984): Nichtlineare Finite-Elemente-Berechnung von Tunnelbauwerken. In: Finite Elemente — Anwendungen in der Baupraxis. W. Ernst u. Sohn, München.

ITA-Working Group on Tunnelling Design (1988): Guidelines for the design of tunnels. Tunnelling and Underground Space Techn. 3 (3), 237—249.

Kielbassa, St. (1989): Stress-strain fields at the tunnelling face and in the tunnel lining (in German). Report Nr. 89-58, Institut für Statik, Technische Universität Braunschweig.

Schikora, K., Ostermeier, B. (1982): Berechnungsmethoden moderner bergmännischer Bauweisen beim U-Bahn-Bau. Bauingenieur 57, 193—198.

Schwartz, C. W., Einstein, H. H. (1978): Improvement of ground support performance by full consideration of ground displacements. In: Proc., Tunnelling and Underground Structures Symposium, TRB Meeting Chicago.

Semprich, S. (1980): Berechnungen der Spannungen und Verformungen im Bereich der Ortsbrust von Tunnelbauwerken im Fels. In: Veröff. Institut für Grundbau, Bodenmechanik und Verkehrswasserbau der RWTH Aachen, H. 8.

Swoboda, G. A., Mertz, W. G. (1987): Rheological analysis of tunnel excavations by means of coupled finite element — boundary element analysis. Int. J. Numer. Analyt. Methods in Geomechanics 11, 115—129.

Authors' address: Dr. S. Kielbassa, Prof. Dr.-Ing. H. Duddeck, Institute for Structural Analysis, Technical University of Braunschweig, Beethovenstraße 51, D-3300 Braunschweig, Federal Republic of Germany.